JOURNAL OF MATERIALS SCIENCE **39** (2004) 3383–3390

Creep effects on early damage initiation in a TBC system

M. Y. ALI, S. Q. NUSIER, G. M. NEWAZ*
Department of Mechanical Engineering, Wayne State University, Detroit, Michigan 48202, USA
E-mail: gnewaz@eng.wayne.edu

High temperature superalloys coated with thermal barrier coating (TBC) may induce creep effects in different layers such as in the bond coat and the thermally grown oxide (TGO) layer. The effects of creep deformation in these layers were investigated on the magnitude of residual stresses in these layers. Results indicated that the residual stress after creep was considerably higher when compared with the stress without creep. This larger value of stresses is likely to enhance the initiation of microcracks and debonding of the TBC leading to spallation. © *2004 Kluwer Academic Publishers*

1. Introduction

The blades in modern gas turbines are subjected to high stress under complex thermal, mechanical, corrosive and erosive conditions [1]. In some parts of the modern gas turbines, temperatures are very high and structures are loaded by static and dynamic forces as well as thermal gradients. To meet these severe environments superalloys are used. However, creep can occur at significant rates in service. Such creep can affect the dimensional stability and prevailing stress states and may lead to eventual failure by creep damage mechanisms. The estimation of creep strains and of damage accumulation become critical consideration in the design of many of the high temperature engine parts [2].

The superalloys are protected from high temperature corrosion by TBCs. The TBC has low thermal conductivity, giving a significant temperature drop from the surface in contact with the combustion gases and the blade alloy. A bond coat is usually required between the TBC and the metal of the blade. A typical system for nickel based superalloy blades uses yttria stabilized zirconia for the TBC and an alloy MCrAlY for bond coat, where M may be Ni or Co or a combination of both. The bond coat improves the adhesion of the TBC to the blade [3–5]. However TBC cannot permanently adhere to the superalloy. Due to environmental and temperature exposure, the TBC may spall off from the superalloy after a certain time.

When the TBC-superalloy system is exposed to high temperature, oxygen seeps through the TBC and depletes aluminum from bond coat. This process creates an Al_2O_3 layer or TGO between the bond coat and TBC layer. These different layers (substrate, bond coat, TGO and TBC) have different thermal expansion coefficients and creep properties. To understand the spallation process of TBC from superalloy it is necessary to correlate the effect of thermal expansion coefficients mismatch as well as creep effect in these layers.

Previously the effect of thermal expansion coefficients mismatch on transient residual stresses has been investigated for both a three-layer and a four-layer cylindrical models [5]. The results from both the analytical and finite element analyses showed a large compressive biaxial stress field (tangential and axial stresses) exists in the oxide layer of the specimen compared to the adjacent layers. The analysis was done without considering any prior creep effect. The present work has been aimed to compute the stress level in bond coat and oxide layers due to creep in these layers, as a step towards the understanding of formation of initial damage that can lead to spallation of TBC from the substrate.

The crack initiation in thermal barrier coatings due to interface asperity was investigated by Nusier and Newaz [6], Ali *et al.* [7] and [8], Chen *et al.* [9], and Chaudhury *et al.* [10]. They used finite element model to determine the variation of residual stresses at a rough bond coat/oxide interface and their results showed that asperities could result in stresses high enough to initiate microcracks.

Brindley and Whittenberger [11] had analyzed stress relaxation of low-pressure plasma-sprayed NiCrAlY alloys. They studied the relaxation of three NiCrAlY alloys at temperatures of 800–1000°C and over a wide range of stresses. They showed that all three bond coat alloys relaxed quite rapidly at temperatures of 900°C and above which may have a potential to affect the TBC life. Also they showed the differences in relaxation of the three alloys, which may offer a possible explanation for the differences in TBC life observed for these bond coats.

*Author to whom all correspondence should be addressed.

Evans *et al.* [3] had analyzed creep effects on the spallation of an alumina layer from a NiCrAlY coating. They showed the spallation by wedge cracking of an alumina from a flat Ni16Cr6AlY coating substrate cooled at various rates from 1100°C. They concluded that slow cooling from the oxidation temperature could lead to useful increases in the high-temperature exposure period before spallation would be initiated during cooling. Padovan *et al.* [12] investigated thermomechanical response of ceramically coated metal parts in elevated thermal environments using improved finite element method for nonlinear elastic-creep. They showed the significant influence of inelastic behavior in generating residual stress fields. Miller and Lowell [13] investigated the failure mechanisms of thermal barrier coatings. They concluded that the coatings fail by delamination prior to visible surface cracking or spalling. Also thermal stresses on heating do not cause this failure rather, under certain conditions, cooling stresses after only a single isothermal heat treatment in an oxidizing environment can cause failure.

Though many researchers have addressed the creep problem in TBC systems, an assessment of the magnitude of residual stresses in different layers and their consequence in damage initiation remains unexplored. Therefore in this investigation focus will be given on the estimation of the stresses in different layers especially in bond coat and the TGO to determine the role of creep on damage initiation in the TBC system.

2. Analytical and numerical modeling

The geometry under consideration is a disk-type four-layer system which includes-substrate, bond coat, TGO and the TBC layer. When the temperature (T) does not vary over the thickness of each layer it can be assumed that the stress and displacement due to heating also do not vary over the thickness. A simplified mechanics of materials approach will be used to determine the layer stresses. In this approach interlaminar stresses are not considered.

3. Viscoplastic deformation and stresses in layers

The in-plane radial stresses as a function of time in a four-layer model of a TBC disk sample can be calculated in the following manner. From ordinary stress-strain relations, for plane stress, with modification for thermal expansion the radial strain ε_r can be given as

$$\varepsilon_r - \alpha \Delta T = \frac{1}{E}(\sigma_r - \nu \sigma_\theta) \tag{1}$$

where, ε_r = Radial strain, σ_r = Radial stress, σ_θ = Tangential stress, α = Thermal expansion coefficient, ν = Poisson's ratio, ΔT = Temperature change and E = Modulus of elasticity.

For a disk, $\varepsilon_r = \varepsilon_\theta$ and $\sigma_r = \sigma_\theta$

So, radial stress (dropping subscript),

$$\sigma = \frac{E}{(1-\nu)}[\varepsilon - \alpha \Delta T] \tag{2}$$

Thus radial stress in each layer is written in the following form

$$\begin{aligned}
\sigma^c(t) &= \frac{E^c}{1-\nu^c}[\varepsilon - \alpha^c(T - T_r)], \\
\sigma^o(t) &= \frac{E^o}{1-\nu^o}\left[\varepsilon - \alpha^o(T - T_r) + \varepsilon^o_{cr}\right] \\
\sigma^b(t) &= \frac{E^b}{1-\nu^b}\left[\varepsilon - \alpha^b(T - T_r) + \varepsilon^b_{cr}\right], \\
\sigma^s(t) &= \frac{E^s}{1-\nu^s}[\varepsilon - \alpha^s(T - T_r)]
\end{aligned} \tag{3}$$

where σ is the radial stress, α is the thermal expansion coefficient and T_r is the stress free temperature, ε_{cr} is the creep strain, the superscript c, o, b and s refers to TBC, TGO, bond coat and substrate, respectively. The well-known temperature-compensated power law for creep can be written as-

$$\dot{\varepsilon} = A\sigma^n \exp\left(-\frac{Q}{RT}\right) \tag{4}$$

where, $\dot{\varepsilon}$ is the strain rate, A is a constant, σ is the stress, n is the stress exponent, Q is the activation energy for deformation, R is the gas constant and T is the absolute temperature. The creep behavior of alumina (TGO) and the bond coat for uniaxial loading were published as follows (bond coat creep model refers to Brindley and Whittenberger [11], and oxide creep model refers to Evans *et al.* [3], Lin and Becher [14])

$$\begin{aligned}
\frac{d\varepsilon^o_{cr}}{dt} &= 1.08 \times 10^{-10} \times \sigma^{o^{2.3}} \exp\left(-\frac{51000}{T}\right), \ \text{s}^{-1}, \\
\frac{d\varepsilon^b_{cr}}{dt} &= 8.96 \times 10^{-15} \times \sigma^{b^3} \exp\left(-\frac{35840}{T}\right), \ \text{s}^{-1}
\end{aligned} \tag{5}$$

But for the present case the effect of creep has been assumed in radial and tangential direction. Thus the creep strain rate for present case can be given as follows [15]

$$\begin{aligned}
\frac{d\varepsilon^o_{cr}}{dt} &= \frac{1.08 \times 10^{-10}}{2} \sigma^{o^{2.3}} \exp\left(-\frac{51000}{T}\right), \ \text{s}^{-1}, \\
\frac{d\varepsilon^b_{cr}}{dt} &= \frac{8.96 \times 10^{-15}}{2} \sigma^{b^3} \exp\left(-\frac{35840}{T}\right), \ \text{s}^{-1}
\end{aligned} \tag{6}$$

PtAl and NiCrAlY are bond coat materials that are widely used in high temperature environment. Since there is no creep model available in the literature for PtAl material, the authors used the creep model for NiCrAlY material to get a broad idea on the effect of creep on stress levels that a component may see under thermal load.

The equilibrium radial force equation for the four layers is

$$\sum F_{\mathrm{r}} = \sigma^{\mathrm{c}}A^{\mathrm{c}} + \sigma^{\mathrm{o}}A^{\mathrm{o}} + \sigma^{\mathrm{b}}A^{\mathrm{b}} + \sigma^{\mathrm{s}}A^{\mathrm{s}} = 0 \qquad (7)$$

where, A represents circumferential edge area and σ represents radial stress in each layer and the superscripts c, o, b, s stands for the TBC, TGO, bond coat and substrate respectively.

Substituting Equation 3 into Equation 7 and solving for ε gives

$$\varepsilon = \frac{\left(\sum_{i=c,o,b,s} \frac{E^{\mathrm{i}}}{1-\nu^{\mathrm{i}}}\alpha^{\mathrm{i}}A^{\mathrm{i}}\right)(T - T_{\mathrm{r}}) - \frac{E^{\mathrm{o}}}{1-\nu^{\mathrm{o}}}A^{\mathrm{o}}\varepsilon^{\mathrm{o}}_{\mathrm{cr}} - \frac{E^{\mathrm{b}}}{1-\nu^{\mathrm{b}}}A^{\mathrm{b}}\varepsilon^{\mathrm{b}}_{\mathrm{cr}}}{\left(\sum_{i=c,o,b,s} \frac{E^{\mathrm{i}}}{1-\nu^{\mathrm{i}}}A^{\mathrm{i}}\right)} \qquad (8)$$

Differentiating Equation 8 gives

$$\frac{\mathrm{d}\varepsilon}{\mathrm{d}t} = \frac{-\frac{E^{\mathrm{o}}}{1-\nu^{\mathrm{o}}}A^{\mathrm{o}}\frac{\mathrm{d}\varepsilon^{\mathrm{o}}_{\mathrm{cr}}}{\mathrm{d}t} - \frac{E^{\mathrm{b}}}{1-\nu^{\mathrm{b}}}A^{\mathrm{b}}\frac{\mathrm{d}\varepsilon^{\mathrm{b}}_{\mathrm{cr}}}{\mathrm{d}t}}{\left(\sum_{i=c,o,b,s} \frac{E^{\mathrm{i}}}{1-\nu^{\mathrm{i}}}A^{\mathrm{i}}\right)} \qquad (9)$$

Now differentiating Equation 3 with respect to time leads to

$$\frac{\mathrm{d}\sigma^{\mathrm{c}}(t)}{\mathrm{d}t} = \frac{E^{\mathrm{c}}}{1-\nu^{\mathrm{c}}}\frac{\mathrm{d}\varepsilon}{\mathrm{d}t}, \quad \frac{\mathrm{d}\sigma^{\mathrm{o}}(t)}{\mathrm{d}t} = \frac{E^{\mathrm{o}}}{1-\nu^{\mathrm{o}}}\left[\frac{\mathrm{d}\varepsilon}{\mathrm{d}t} + \frac{\mathrm{d}\varepsilon^{\mathrm{o}}_{\mathrm{cr}}}{\mathrm{d}t}\right],$$
$$\frac{\mathrm{d}\sigma^{\mathrm{b}}(t)}{\mathrm{d}t} = \frac{E^{\mathrm{b}}}{1-\nu^{\mathrm{b}}}\left[\frac{\mathrm{d}\varepsilon}{\mathrm{d}t} + \frac{\mathrm{d}\varepsilon^{\mathrm{b}}_{\mathrm{cr}}}{\mathrm{d}t}\right], \quad \frac{\mathrm{d}\sigma^{\mathrm{s}}(t)}{\mathrm{d}t} = \frac{E^{\mathrm{s}}}{1-\nu^{\mathrm{s}}}\frac{\mathrm{d}\varepsilon}{\mathrm{d}t} \qquad (10)$$

Substituting Equations 6 and 9 into Equation 10 gives a system of first order differential equations, which can be integrated numerically to obtain the radial stress in each layer as function of time. Upon cooling, these equations will give the final residual stress.

4. Finite element stress analysis

The nickel-based superalloy substrate Rene N5 had a thickness of 3.175 mm, the bond coat layer thickness is 0.036 mm, the thermally grown oxide (TGO, aluminum oxide) layer thickness is 0.012 mm, the TBC thickness is 0.127 mm, and the radius of the specimen is 12.7 mm. These dimensions are shown in Fig. 1a and the properties of these four layers are given in Table I. The analysis was done for a model case where the bond coat was a diffusion aluminide PtAl alloy, which protects the alloy substrate from oxidation and bonds very well to both the alloy substrate and the outer EB-PVD thermally insulating TBC layer. The outer layer of the TBC was 8 wt% yttria stabilized zirconia (YSZ). It was assumed that the specimen has been pre-exposed to the oxidizing environment to collect the mentioned oxide layer thickness. The specimen was cooled down from a processing temperature of 1000°C to room temperature 25°C and then elevated to a temperature of 1177°C and held at that temperature until the radial stresses in bond coat and oxide layers die out to zero. Then the specimen is again cooled down to temperature 25°C.

The finite element model was used for the case of four layers using ABAQUS with user defined creep laws for bond coat and oxide layers. A half model was used since the specimen is axisymmetric. Eight-node axisymmetric biquadratic quadrilateral element type was used. Along the axisymmetric axis (axial), the nodes are allowed to move in the axial direction only.

5. Experimental aspects

In the previous damage accumulation research work in the authors laboratory at Wayne State University a disk type sample (diameter 25.4 mm, superalloy substrate Rene N5 thickness 3.175 mm, PtAl bond coat thickness 0.36 mm and TBC thickness 0.127 mm) was tested for two cycles. Each cycle consisted of ramping from 200 to 1177°C in 9 min, 45 min holding time at 1177°C and then ramping down to 200°C in 10 min. Thus the total holding time was 5.4×10^3 s. The specimen was then sectioned and metallurgically polished

TABLE I Material properties [16]

Material	Temp. (°C)	Young's modulus (GPa)	Poisson's ratio	Coefficient of thermal expansion ($^{\circ}C^{-1}$)	Coefficient of thermal conductivity (W/m/k)	Coefficient of thermal diffusivity (m^2/s)
Substrate	0	176.8	0.24973	13.85×10^{-6}	–	–
	22	175.8	0.25	13.91×10^{-6}	7	2×10^{-6}
	566	150.4	0.25658	15.36×10^{-6}	13	3.4×10^{-6}
	1149	94.01	0.32237	19.52×10^{-6}	22	324×10^{-6}
Bond coat	0	138.6	0.27	15.15×10^{-6}	–	–
	22	137.9	0.27	15.16×10^{-6}	25	8×10^{-6}
	566	124	0.27	15.37×10^{-6}	50	13.56×10^{-6}
	1149	93.8	0.27	17.48×10^{-6}	65	15.52×10^{-6}
Oxide	0	387.8	0.257	5.92×10^{-6}	–	–
	22	386	0.257	6×10^{-6}	36	19×10^{-6}
	566	347.6	0.257	8×10^{-6}	9.9	–
	1149	312.1	0.257	8.9×10^{-6}	5.89	–
TBC	0	28.5	0.25	9.97×10^{-6}	–	–
	22	27.6	0.25	10.01×10^{-6}	1	5×10^{-7}
	566	6.9	0.25	11.01×10^{-6}	0.96	3.51×10^{-7}
	1149	84	0.25	1301×10^{-6}	1	3.43×10^{-7}

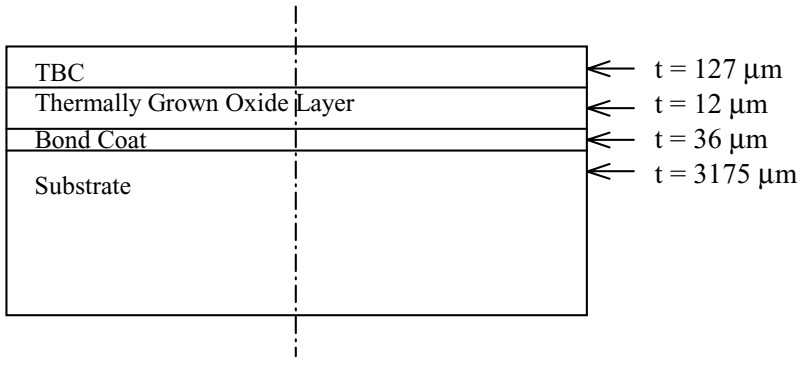

(a)

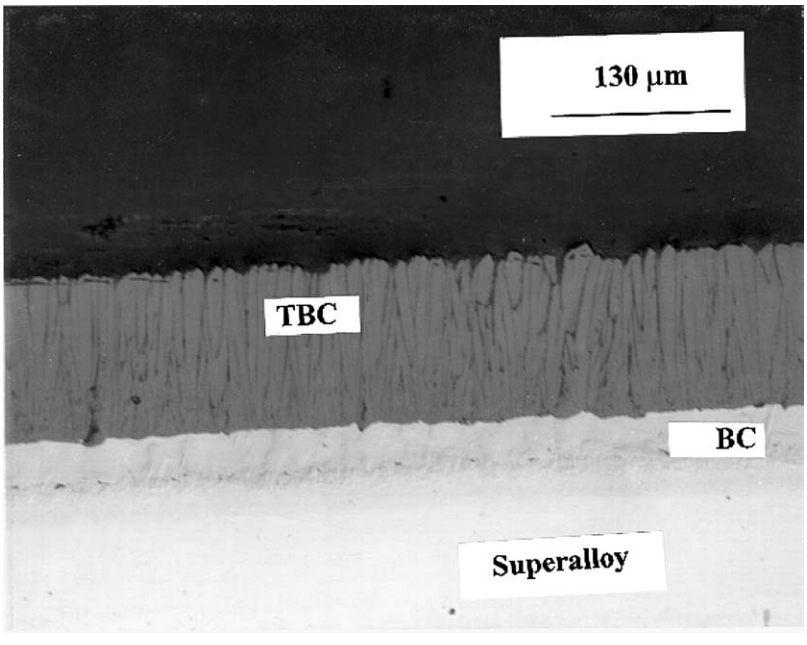

(b)

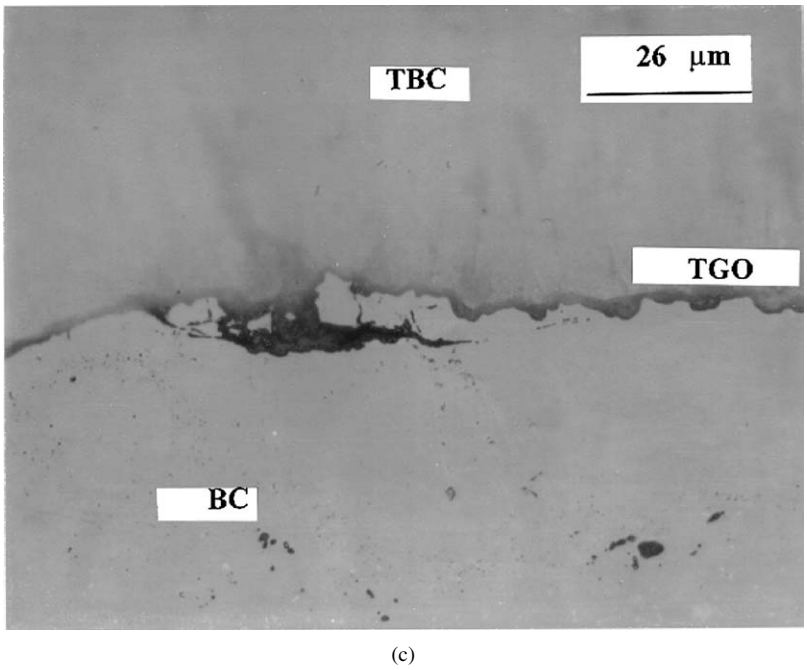

(c)

Figure 1 (a) Dimensions of the four-layer disk specimen (radius 12.7 mm). (b) Shows an optical micrograph of an untested thermal barrier coated sample. Thermally grown oxide (TGO) layer and/or interfacial separation was absent at the bond coat/top coat (TBC) interface. (c) Shows an optical micrograph of a tested thermal barrier coated sample. Thermally grown oxide (TGO) layer and/or interfacial separation were seen at the bond coat/top coat (TBC) interface. The sample was thermally cycled to 2 cycles (each cycle consists of ramping from 200 to 1177°C in 9 min, 45 min holding time at 1177°C and then ramp down to 200°C in 10 min).

to view the layers by optical microscopy. The optical micrograph of the tested thermal barrier coated sample showed a thermally grown oxide (TGO) layer. An interfacial separation was seen at the bond coat/TBC interface. This is shown in Fig. 1c. Obviously the oxide layer that has been formed at this period of time, undergone the creep and the partial separation or cracking may be due the large stress development in the bond coat and oxide layer due to the creep effect.

6. Results

When the specimen was cooled down from a processing temperature of 1000°C to a temperature of 25°C and then elevated to a temperature of 1177°C, the stresses in bond coat and TGO were tensile stresses (refer to point 'b' in Figs 2 and 3 respectively). Analysis showed that if the specimen were cooled from 1177 to 25°C without considering the creep effect the final stress would be the point 'NC*' in Figs 2 and 3 i.e., same stress as point 'a' in the corresponding Fig. But due to creep the stress at that higher temperature (1177°C) decayed with time. The specimen was then cooled from that point (refer to point 'c' in Figs 2 and 3) but the final stresses were not at the point 'NC*' as mentioned above. The final stresses were below the point 'NC*' (refer to point 'd' in Figs 2 and 3), which showed larger compressive stresses. This can be explained since due to creep at 1177°C the stresses decayed to zero in different layers of the superalloy system. The disc behaves as if the processing temperature were 1177°C rather than 1000°C. This is the case at point 'c' (refer to Figs 2 and 3), and higher processing temperature would give higher compressive residual stresses upon cooling to 25°C. This argument was verified analytically.

For the creep laws that have been used, the stresses in bond coat decayed very quickly compared to the oxide layer. Fig. 2 shows bond coat radial stress versus log time. To show the stresses at zero time the value 1 is added with each time scale for convenience. From Fig. 2 it can be shown that at elevated temperature the radial stress in bond coat decays to 1% at time 62 s. Fig. 3 shows the TGO layer radial stress versus log time. Here also to show the stresses at zero time the value 1 is added with each time scale for convenience. From Fig. 3 it can be shown that at elevated temperature the radial stress in TGO layer decays to 1% at time 8.09×10^5 s. The specimen was held at elevated temperature for 1×10^6 s to get radial stress in the TGO close to zero. Then it was cooled to temperature 25°C. The compressive residual radial stresses in bond coat and TGO layer were found to be 68 and 30% respectively more than if there were no creep. From analytical investigation it has been found that if the specimen was cooled to 25°C before the complete decay of stresses at holding temperature, the final stresses would be at a level between points 'a' and 'd' of Figs 2 and 3.

There could be a little variation in measuring creep law parameters value (A, Q and n) for TGO and bond coat from experiment to experiment. This variation in parameters value may affect the stress level prediction for the spallation of TBC from the substrate. This necessitates checking the sensitivity of final stress to the

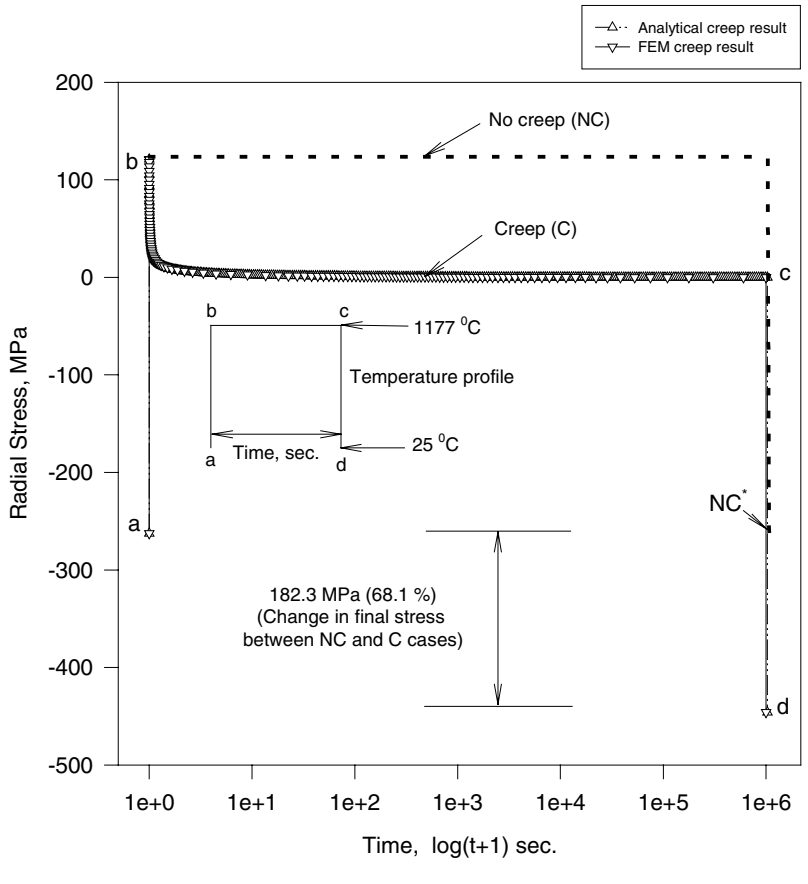

Figure 2 Thermal loading cycle and corresponding stress vs. time profile in bond coat for disk specimen. Analytical and FEM results matches extremely well (NC* represents the final value for NC analysis).

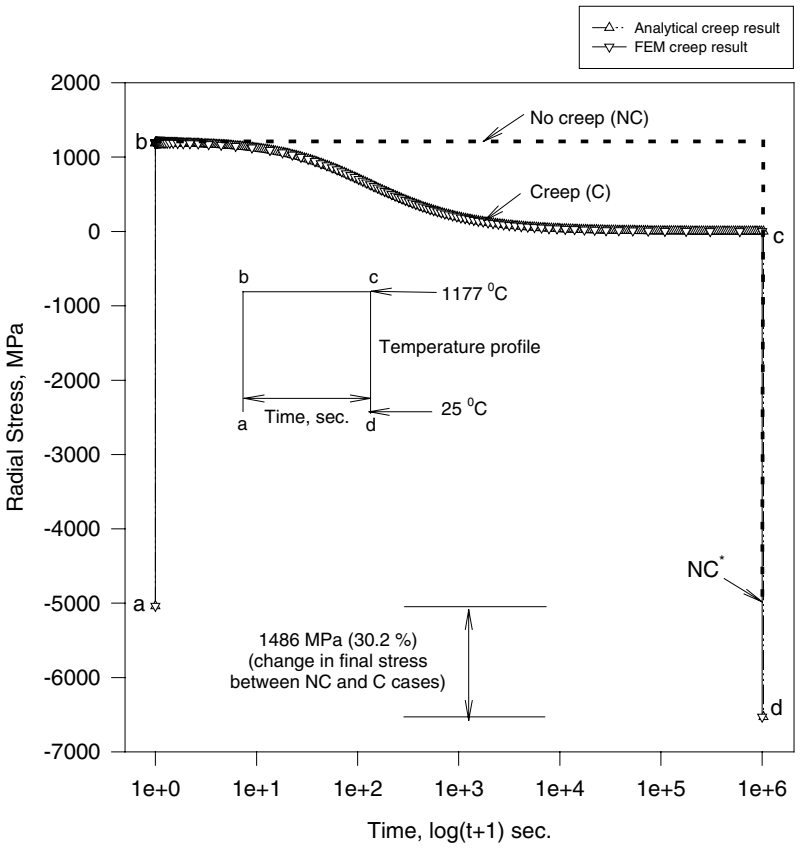

Figure 3 Thermal loading cycle and corresponding stress vs. time profile in Oxide layer for disk specimen. Analytical and FEM results matches extremely well (NC* represents the final values for NC analysis.).

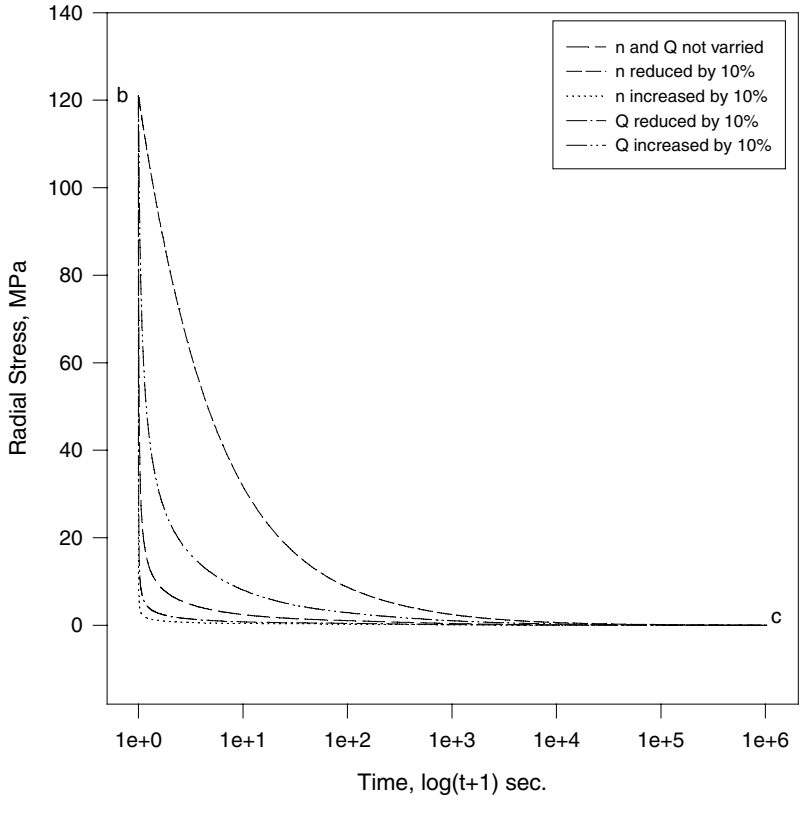

Figure 4 Effect of bond coat creep parameters (n and Q) on radial stress decay in the same layer (points 'b' and 'c' are the same points as in Fig. 2).

creep law parameters. The effects of variation of n and Q on the creep stress of the corresponding layer were shown in Fig. 4 for bond coat and Fig. 5 for oxide layer. From Figs 4 and 5 it is obvious that the stress decay is more sensitive to the variation of n rather than that of Q. The time required for complete stress decay was less for higher value of n and more for lower value of n, which was reverse for Q (n and Q was varied 10% in

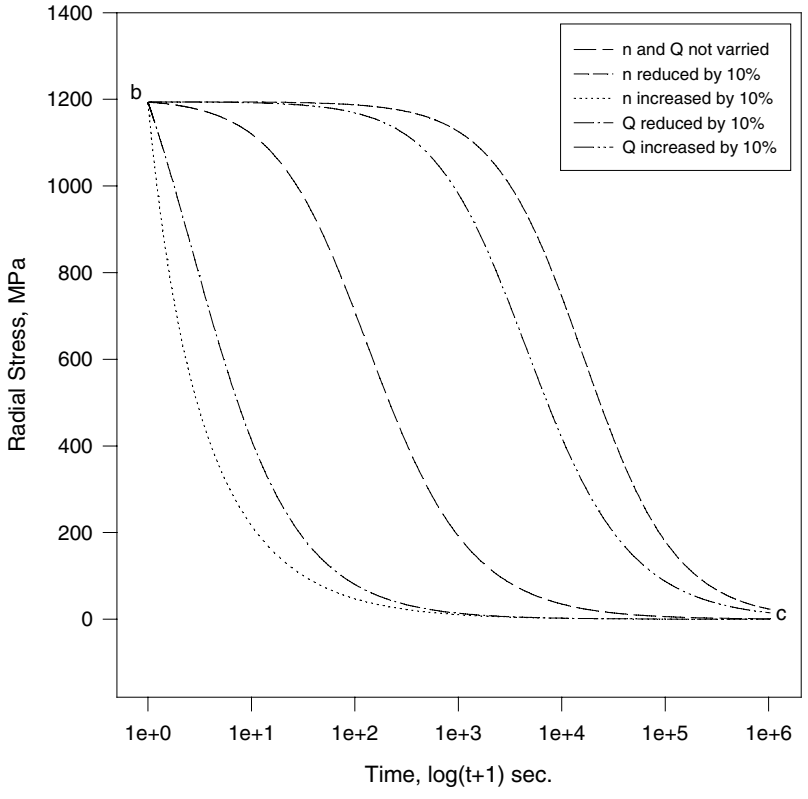

Figure 5 Effect of oxide layer creep parameters (n and Q) on radial stress decay in the same layer (points 'b' and 'c' are the same points as in Fig. 3).

the analysis). For the case of incomplete stress decay, if the temperature were lowered at that time the final stress would be in the stress level between points 'a' and 'd' of the Figs 2 and 3.

7. Summary and conclusions

1. Radial stress in the TGO layer is substantially higher compared with the radial stress in the bond coat (one order of magnitude) and plays a critical role in early damage initiation in TBC coated superalloy system. Compressive stress can be high (∼6400 MPa) indicating that microcracking within the TGO layer is a definite possibility since TGO compressive strength for pure Al_2O_3 is ∼3860 MPa (for zero porosity 100% polycrystalline alumina)

2. Using creep laws from literature for bond coat and TGO, a 30 percent increase in compressive stress is expected in TGO. This enhances the possibility of early damage initiation in TGO/bond coat interface based on the compressive strength of pure Al_2O_3 as given in 1.

3. Experimental results confirmed that for two cycles early damage occurred. The analytical and numerical results showed that the creep effect is not negligible for that time span.

4. Analytical and FEA results for creep match very well indicating confidence in the solution.

5. A Parametric study of n and Q showed the stress decay is more sensitive to the variation of n rather than that of Q. The time required for complete stress decay is less for higher values of n and more for lower value of n (10% varied in the analysis). For Q a reverse result is expected.

Acknowledgment

Funding for this research was provided through a grant (#F49620-98-1-0390) from the Air Force Office of Scientific Research (AFOSR). Dr. Ozden Ochoa was the program monitor. Discussion and interaction with Dr. P. K. Wright of GEAE is gratefully acknowledged.

References

1. N. CZECH, W. EßER and F. SCHMITZ, *Mater. Sci. Techn.* **2** (1986) 244.
2. R. W. EVANS and B. WILSHIRE, *ibid.* **3** (1987) 701.
3. H. E. EVANS, A. STRAWBRIDGE, R. A. CAROLAN and C. B. PONTON, *Mater. Sci. Engng.* A **225** (1997) 1.
4. G. M. NEWAZ, S. Q. NUSIER and Z. A. CHAUDHURY, *ASME, J. Engng. Mater. Techn.* **120**(2) (1998) 149.
5. S. Q. NUSIER and G. M. NEWAZ, *ASME , J. Appl. Mech.* **65** (1998) 001.
6. *Idem*., "Crack Initiation In Thermal Barrier Coatings Due to Interface Asperity," in Proceedings of the Eighth Japan-U.S. Conference on Composite Materials (1998) p. 417.
7. Y. ALI, S. Q. NUSIER and G. M. NEWAZ, *Intern. J. Solids Struct.* **38** (2001) 3329.
8. Y. ALI, X. Q. CHEN and G. M. NEWAZ, *J. Mater. Sci.* **36** (2001) 1.
9. X. Q. CHEN and G. M. NEWAZ, *J. Mater. Sci. Lett.* **20** (2001) 93.
10. Z. A. CHAUDHURY, G. M. NEWAZ, S. Q. NUSIER, T. AHMED and R. L. THOMAS, *J. Mater. Sci.* **34** (1999) 2475.
11. W. J. BRINDLEY and J. D. WHITTENBERGER, *Mater. Sci. Engng.* A **163** (1993) 33.
12. J. PADOVAN, D. DOUGHERTY, R. HENDRICKS, M. J. BRAUN and B. T. F. CHUNG, *J. Therm. Stress.* **7** (1984) 51.
13. R. A. MILLER and C. E. LOWELL, *Thin Solid Films* **95** (1982) 265.

14. H. T. LIN and P. F. BECHER, *J. Amer. Ceram. Soc.* **73** (1990) 1378.
15. J. M. CLARKE and J. F. BARNES, in "Stress Redistribution Caused by Creep In A Thick Walled Circular Cylinder Under Axial and Thermal Loading," edited by A. I. Smith and A. M. Nicolson, *Advances in Creep Design* (John Wiley & Sons, Inc., New York, 1971) p. 387.
16. P. K. WRIGHT, Private Communication, General Electric Aircraft Engines, Evendale, OH, 1995.

Received 17 April 2003
and accepted 28 January 2004